Journal of Hydrology 401 (2011) 1–13

Contents lists available at ScienceDirect

Journal of Hydrology

journal homepage: www.elsevier.com/locate/jhydrol

Towards improved criteria for hydrological model calibration: theoretical analysis of distance- and weak form-based functions

V. Guinot *, B. Cappelaere, C. Delenne, D. Ruelland

HydroSciences Montpellier UMR 5569 (CNRS, IRD, UM1, UM2), Université Montpellier 2, CC MSE, 34095 Montpellier Cedex 5, France

ARTICLE INFO

Article history:
Received 17 December 2009
Received in revised form 21 December 2010
Accepted 3 February 2011

This manuscript was handled by P. Baveye, Editor-in-Chief

Keywords:
Model performance evaluation
Calibration
Objective function
Mean squared error
Nash–Sutcliffe efficiency
Conceptual hydrological model

SUMMARY

Calibrating conceptual hydrological models is often done via the optimization of objective functions serving as a measure of model performance. Most of the objective functions used in the hydrological literature can be classified into distance- and weak form-based objective functions. Distance- and weak form-based objective functions can be seen respectively as generalizations of the square error and balance error. An analysis of the objective functions shows that: (i) the calibration problem is transformed from an optimization problem with distance-based objective functions into a root finding problem for weak form-based functions; (ii) weak form-based objective functions are essentially less prone to local extrema than distance-based functions; (iii) consequently, they allow simple gradient-based methods to be used; (iv) parameter redundancy can be assessed very simply by superimposing the contour lines or comparing the gradients of two objective functions of similar nature in the parameter space; and (v) simple guidelines can be defined for the selection of the calibration variables in a conceptual hydrological model. The theoretical results are illustrated by two simple test cases. Weak form-based approaches offer the potential for better-posed calibration problems, through the use of a number of independent criteria that matches the dimension of the identification problem. In contrast with distance-based objective functions, they do not have the inconvenience of solution non-uniqueness. Finally, the need for models with internal variables bearing a physical meaning is acknowledged.

1. Introduction

Calibration is recognized as an essential step in the operation of conceptual, hydrological models. It is classically translated into an optimization problem, whereby an objective function expressing the goodness-of-fit of the model, must be minimized or maximized depending on the definition. Although several authors have pointed out the importance of seeing calibration as a multi-objective optimization exercise using variables and criteria of different natures (Yapo et al., 1998; Gupta et al., 1998; Meixner et al., 1999), it is still conducted as a single-objective optimization procedure in a vast majority of practical applications. The same holds for model performance assessment that is often performed using the same type of objective functions as those used in the calibration process. Such analyses are usually performed on the basis of empirical considerations, for which formal foundations are lacking. Although there is a commonly shared perception of the calibration/validation exercise in the hydrological community, this lack of theoretical bases often does not allow reliable guidelines to be derived.

The present paper focuses on two types of objective functions: so-called distance-based and weak form-based (or integral) objective functions (see Section 2 for a definition). The purpose is to analyse the behaviour of such functions and to determine under which conditions some may be better-suited than others. The choice of the model variable(s) to be used in the calibration process is also discussed. The behaviour of distance-based and weak form-based objective functions is analysed theoretically and illustrated by two simple case studies.

Distance-based objective functions represent the vast majority of objective functions used in hydrological modelling (Kavetski et al., 2006b; Schaefli and Gupta, 2007). Distances may be defined for the original (Kavetski et al., 2006a) or transformed variables. In Hogue et al. (2000, 2006) and Kavetski et al. (2006b), a logarithmic transformation error is presented. The Nash–Sutcliffe Efficiency (NSE) criterion (Nash and Sutcliffe, 1970), based on a Square Error (SE) measure of distance, is definitely the most widely used objective function in hydrological modelling. It is a normalized variant of the Least Square Estimator (LSE), and gives equivalent information to that given by the Mean Square Error (MSE), or Root Mean Square Error (RMSE). A number of theoretical justifications can be provided for the NSE. For instance, the NSE optimum corresponds to the Maximum Likelihood Estimator for a homoscedastic, Gaussian distribution of model errors (Cacuci, 2003). This justifies

* Corresponding author. Tel.: +33 (0)4 67 14 90 56; fax: +33 (0)4 67 14 47 74.
E-mail address: guinot@msem.univ-montp2.fr (V. Guinot).

0022-1694/$ - see front matter © 2011 Elsevier B.V. All rights reserved.
doi:10.1016/j.jhydrol.2011.02.004

its use in model performance evaluation and uncertainty assessment techniques such as the GLUE approach (Beven and Binley, 1992; Beven, 1993; Romanowicz and Beven, 2006). The NSE can also be seen as the sum of three indicators (Murphy, 1988; Weglarczyk, 1998) involving the correlation coefficient between the measured and modelled variable, as well as a measure of conditional and unconditional bias. Gupta et al. (2009) provided another decomposition of the NSE involving the correlation, the bias and a measure of relative variability in the measured and modelled signals.

The NSE is not the only possible measure of distance. In Perrin et al. (2001) the Mean Absolute Error (MAE) is proposed. It can be normalized into a dimensionless index such as the volumetric efficiency (Criss and Winston, 2008). In Legates and McCabe (1999), the Nash–Sutcliffe efficiency criterion is generalized by replacing the square of the deviations with a power to be adjusted by the modeller. The purpose is to balance the larger weight given to large flow values (that are often measured with the larger imprecision) by using a power smaller than 2 (Krause et al., 2005). Taylor (2001) proposed alternative skill functions that increase with better correlation or modelled variance while giving those varying relative importance. To overcome the deficiency of the original GLUE method in reflecting modelling uncertainty, more formal derivations of likelihood functions (e.g., Schoups and Vrugt, 2010) or empirical adaptations of the approach (Cappelaere et al., 2003; Xiong and O'Connor, 2008) have been proposed.

Lin and Wang (2007) use the inverse of the SE and the NSE for computing respectively the efficiency of chromosoms and the objective function in a genetic, global optimization algorithm. Several objective functions may also be defined for low flows or peak flow events, so as to allow for multi-objective calibration (Madsen, 2000; Madsen et al., 2002). Multi-objective calibration may also be carried out using variables of different natures (such as response signatures, see Pokhrel et al. 2009; Seibert and McDonnell, 2002). A review of multi-objective calibration approaches can be found in Efstratiadis and Koutsoyiannis (2010). Conversely, multiple distance-based objective functions may be aggregated into a single one (Madsen et al., 2002; Cappelaere et al., 2003; Schoups et al., 2005). Additional information may be brought by integral criteria such as the bias (Hogue et al., 2006; Schoups et al., 2005), volume error (Madsen, 2000), also called Cumulative Error (CE) (Perrin et al., 2001).

Distance-based objective functions are well-known to introduce local minima in model response surfaces (Freedman et al., 1998; Skahill and Doherty, 2006; Xiong and O'Connor, 2000). In Freedman et al. (1998), distance-based objective functions such as the Least Squares Estimator (LSE) and the Heteroscedastic Maximum Likelihod Estimator (HMLE) are shown to introduce local extrema in the objective functions of a sediment transport model, thus introducing the need for global optimization or objective function exploration algorithms (see e.g. Brazil and Krajewski, 1987; Goldberg, 1989; Nelder and Mead, 1965; Skahill and Doherty, 2006; Duan et al., 1992). Modelling experiments where the LSE and HMLE were used to calibrate and validate different models on the same data indicated that the choice of the objective function plays a significant role on the final, calibrated parameter values (Gan et al., 1997).

Weak form-based objective functions are somewhat less popular, as indicated by the inventory in Appendix A. The best-known weak form-based objective functions are the Cumulative Error (CE) (Perrin et al., 2001), also called Volume Error (Madsen, 2000), and the Balance Error (BE) (Perrin et al., 2001). The BE is nothing but a scaled version of the CE. The variable used in the CE and BE is usually the discharge at the outlet of the modelled catchment. The optimal value of the BE or CE is zero. The BE or CE may be used either as a constraint (typically, CE = 0) in a single-objective optimization process or as an objective function in a multiple objective calibration exercise (see e.g. Ruelland et al., 2009). That the BE or CE is only a particular case and can be generalized so as to generate a wider family of weak form-based objective functions has been little investigated in the literature. This is one of the aspects explored in this paper.

The question also arises of whether using additional variables (such as model internal variables) allows the calibration problem to be better constrained. This is of particular interest as new sources of information are now available to account for storage observations in conceptual modelling (e.g., Werth et al. 2009; Winsemius et al., 2006).

The present paper deals with objective functions for conceptual hydrological models that can be described by first-order differential equations. The main objectives are to (i) generalize the formulation of weak form-based objective functions, (ii) analyze the respective behaviour of distance-based and weak form-based objective functions and the resulting degree of difficulty and reliability in the calibration exercise, (iii) investigate whether certain model variables (e.g. internal variables or output fluxes) bring more information than others in the calibration of model parameters.

In Section 2, distance-based and weak form-based objective functions are defined and a mathematical justification is proposed for them.

In Section 3, the behaviour of such objective functions when applied to conceptual models is analyzed. Weak form-based objective functions are shown to be more monotone and less prone to local extrema than distance-based objective functions. Simple rules for detecting parameter redundancy are given and guidelines are provided for the choice of calibration variables.

Sections 4 and 5 provide two application examples. In Section 4, a single reservoir model is considered and synthetic time series are used in order to avoid any possible site-dependent bias. In Section 5, a three-reservoir model is applied to a Western African catchment.

Section 6 is devoted to a discussion and concluding remarks. Weak form-based approaches are shown to offer the potential for better-posed calibration problems. This can be achieved by defining a number of independent functions that matches the dimension of the identification problem.

2. Objective function definition

2.1. Introduction

Consider a model in the form

$$\frac{dU}{dt} = f(U, \varphi, t) \tag{1}$$

where U is the state variable, t is the independent variable (in hydrological modelling, the time coordinate), φ a parameter to be calibrated, and f is a known function of U, t and φ. The standard calibration approach consists in comparing the variable U or a function $F(U)$ of U with an observed variable $V(t)$ over a certain domain $\Omega = [t_1, t_2]$ and adjusting φ in such a way that U (or $F(U)$) is «as close as possible» to V. In what follows, the function F is assumed to be a monotone function of U and φ. This assumption is verified by many models such as conceptual models, where F can be, for instance, taken as the discharge Q that is a function of water storage U (see Section 4). In the general case, where F is not necessarily a physical function but any scaling function, it is chosen monotone in order to avoid several values of $F(U)$ for a given value of U.

The question then arises of how the closeness between U (or $F(U)$) and V should be assessed via an objective function. If the

model is perfect, the output U or $F(U)$ reproduces exactly the variations of the measured variable V, that is, $U = V$ or $F(U, \varphi) = V$ for all t over the time interval Ω (the issue of data accuracy and measurement precision is not considered in the present work).In practice, this is never the case and the purpose of the calibration procedure is to bring the difference $(U - V)$ or $(F(U, \varphi) - V)$ as close to zero as possible. Two types of objective functions are examined hereafter: distance-based and weak form-based objective functions.

2.2. Distance-based objective function

The distance-based approach is the most widely used in hydrological modelling. In this approach, the objective function is defined as one of the following two functions

$$J = a + b\|e\|_\Omega = a + b\|U - V\|_\Omega \tag{2a}$$
$$J = a + b\|e\|_\Omega = a + b\|F(U, \varphi) - V\|_\Omega \tag{2b}$$

where a and b are respectively an offset and a scaling constant, e is the modelling error, defined as the difference between the modelled and observed variable, and the operator $\|\|$ has the properties of a norm (Courant and Hilbert, 1953):

$$u(t) = 0\ \forall t \in \Omega \iff \|u\|_\Omega = 0 \tag{3a}$$
$$\|ku\|_\Omega = |k|\|u\|_\Omega \quad \forall k \in \Re \tag{3b}$$
$$\|u + v\|_\Omega \leqslant \|u\|_\Omega + \|v\|_\Omega \tag{3c}$$

In other words, the objective function J provides a measure of the distance between the model output U or $F(U, \varphi)$ and the measurement V. Property (3a) provides a fundamental justification to the distance-based approach. If the model is perfect (that is, if it allows the observed variable V to be reproduced exactly), the error e is zero over Ω and the objective function J is a, which is the extreme possible value. Conversely, if J is a, the model is perfect. In practice, J is never equal to a because the model is not perfect. However, J can be optimized by adjusting φ suitably, hence the need for optimization procedures.

If the data used in the calibration process is discrete (e.g. daily, weekly or monthly hydrographs), the norm is computed using a discrete sum. If the data can be considered a continuous function of time, the norm is computed using an integral. In what follows, only continuous functions of time will be considered for the sake of conciseness. However, the conclusions drawn for such functions remain valid for discrete model outputs.

Examples of distance-based objective functions are given in Appendix A. The Nash–Sutcliffe Efficiency (NSE), the Square Error (SE), the Root Mean Square Error (RMSE), the Mean Absolute Error (MAE), the Volumetric Efficiency (VE) or the Generalized Nash–Sutcliffe Efficiency (GNSE) presented in the appendix can be recast in the form (2) via a proper definition of the constants a and b. The NSE gives exactly the same information as the SE, only the offset and scaling differs. The same remark holds for the MAE and VE.

Note that:

(R1) Eq. (2a) is a particular case of Eq. (2b). Eq. (2a) provides a measure of distance between the modelled state variable U in the model and the measured one, V. It is recalled that, in most applications of hydrological models, however, the variable used in the objective function is not the state variable U itself (e.g. the water depth in one of the model reservoirs) but a function of it (e.g. the output discharge). Consequently, Eq. (2b) is the most widespread form of objective function used.

(R2) The function F in Eq. (2b) may also include a transformation in the variables. For instance, in some applications the logarithm, or square root of the discharge, is deemed a more appropriate variable than the discharge itself because it gives more weight to low flows.

(R3) The objective function may be defined for a specific range of the observed (or modelled) variables. For instance, two different values of the objective function may be computed over a given period, one for low flows and another one for high flows (see e.g., Perrin et al., 2001). In this case, a weighting function $w(V)$ is used, which is nonzero only over a subset of Ω and the norm can be written as

$$\|e\| = \left[\int_\Omega w(V)|F(U, \varphi) - V|^p \mathrm{d}t\right]^{1/p}, \quad p > 0 \tag{4a}$$
$$\|e\| = \left[\sum_i w(V_i)|F(U_i, \varphi) - V_i|^p\right]^{1/p}, \quad p > 0 \tag{4b}$$

where $w(V)$ is a weighting function, equal to 0 or 1 depending on whether V is considered to belong to the category of low [high] flows, and i is the record number. Eqs. (4a) and (4b) are respectively the continuous and discrete versions of the norm. In what follows, the continuous form (4a) will be used for the sake of notation consistency, but the reader should keep in mind that the discrete form (4b) may be used instead without loss of generality. The conclusions derived using the formulation (4a) also hold for the formulation (4b) of the objective function.

(R4) In Eq. (4), any positive weighting function w may be used over Ω. The simplest possible case is $w = \mathrm{Const}$, but non constant, positive functions of V, U, $F(U)$ and/or t may also be considered.

(R5) The distance-based objective functions presented in Appendix A are particular cases of Eq. (4), where the norm of the modelling error is defined as a power of its absolute value, called a p-norm. In the NSE and SE objective functions, $p = 2$, while $p = 1$ in the MAE and VE. In the GNSE, p may be set to any value, which does not necessarily have to be an integer. However, other definitions may be proposed for the norm. For instance the maximum of the modelling error over the domain Ω also verifies the definition (3a) for a norm:

$$\|e\| = \max_\Omega[|F(U, \varphi) - V|] \tag{5}$$

Note that the power $1/p$ in Eqs. (4a and b) is not indispensable but allows Eq. (3b) to be verified.

(R6) The calibration process is an optimization process.

2.3. Weak form-based objective function

The weak form-based approach uses the property

$$e(t) = 0 \forall t \in \Omega \iff \int_\Omega eV\ \mathrm{d}t = 0 \quad \forall v(t) \tag{6}$$

where $v(t)$ is a function defined over Ω. In what follows, v is defined as $v = w|e|^{p-1}$ for the sake of similarity with Eq. (4). This leads to the following definition for the weak form-based objective function

$$J_p = a + b\int_\Omega w|e|^{p-1}e\ \mathrm{d}t, \quad p \geqslant 0 \tag{7}$$

where a and b are respectively an offset and scaling parameter, and w is a positive weighting function defined over Ω. The Volume Error/Cumulative Error (CE) and the Balance Error (BE) presented in Appendix A are particular cases of Eq. (7) with $p = 0$ and $w(t) = 1$. In contrast with the distance-based approach, the objective function defined in Eq. (7) is not necessarily positive.

The following remarks may be made:

(R7) Eq. (7) is a particular case of the integral expression in (6) obtained for the specific choice $v = w|e|^{p-1}$ of the weighting function. Other formulations may be considered for v. The formula proposed in (7) has the advantage that it bears similarity with familiar distance-based objective functions (only an absolute value operator needs to be modified).

(R8) The calibration procedure is transformed into a root finding problem. The most desirable value for the objective function is the offset value a.

3. Sensitivity analysis for conceptual models

3.1. Assumptions – preliminary remarks

Consider a model obeying Eq. (1). The specific form of (1) examined hereafter is

$$\frac{\mathrm{d}U}{\mathrm{d}t} = R(U,t,\varphi) - g(U,\varphi) \tag{8a}$$

$$U(t_1) = U_1 \tag{8b}$$

where g is a known function of U and φ, and R is a known function of U, t and φ. In conceptual models, R represents the recharge, or inflow, and g represents the outflow.

The following assumptions are made:

(A1) R and g are positive over Ω:

$$R(t,\varphi) \geqslant 0 \quad \forall t \in \Omega \tag{9a}$$

$$g(t) \geqslant 0 \quad \forall t \in \Omega \tag{9b}$$

(A2) The difference $R - g$ is a decreasing function of U and a monotone function of φ:

$$\frac{\partial}{\partial U}(R-g) \leqslant 0 \quad \forall U \tag{10a}$$

$$\operatorname{sgn}\left[\frac{\partial}{\partial \varphi}(R-g)\right] = \text{Const} \quad \forall \varphi \tag{10b}$$

(A3) There always exists a positive, steady state solution, that is, a value of U_0 for which the outflow g is equal to the inflow R:

$$\exists U_0 > 0, \quad g(U_0,\varphi) = R(U_0,t,\varphi) \quad \forall (t,\varphi) \tag{11}$$

(A4) $U(t_1)$ is positive:

$$U(t_1) \geqslant 0 \tag{12}$$

Assumptions (A1)–(A4) are typical of conceptual models (see Section 4). When these assumptions hold, U is positive over the domain Ω (see Section B.1 in Appendix B for the proof).

The sensitivity of U with respect to φ is defined as $s = \partial U/\partial\varphi$. The governing equation for s is obtained by differentiating (8) with respect to φ:

$$\frac{\mathrm{d}s}{\mathrm{d}t} = \frac{\partial}{\partial\varphi}(R-g) + s\frac{\partial}{\partial U}(R-g) \tag{13a}$$

$$s(t_1) = 0 \tag{13b}$$

where the initial condition $s(t_1) = 0$ is derived considering that $U(t_1) = U_1$ is known and does not change with φ.

It can be shown (see Section B.2 in Appendix B for the proof) that if $\partial R/\partial\varphi - \partial g/\partial\varphi$ keeps the same sign for all t, s has the same sign as $\partial R/\partial\varphi - \partial g/\partial\varphi$:

$$\left.\begin{array}{l} \frac{\partial R}{\partial\varphi} - \frac{\partial g}{\partial\varphi} \leqslant 0 \quad \forall t \in \Omega \\ s(t_1) = 0 \end{array}\right\} \Rightarrow s(t) \leqslant 0 \quad \forall t \in \Omega \tag{14a}$$

$$\left.\begin{array}{l} \frac{\partial R}{\partial\varphi} - \frac{\partial g}{\partial\varphi} \geqslant 0 \quad \forall t \in \Omega \\ s(t_1) = 0 \end{array}\right\} \Rightarrow s(t) \geqslant 0 \quad \forall t \in \Omega \tag{14b}$$

3.2. Distance-based objective function

Consider a distance-based objective function using the definition (4) for the norm of the modelling error:

$$J_p = a + b\int_\Omega w\,|F(U,\varphi) - V|^p\,\mathrm{d}t \tag{15}$$

where $U(t)$ obeys (8), F is a monotone function of U as mentioned in Section 2.1 and w is a strictly positive weighting function over the domain Ω. Then the derivative of the objective function with respect to φ is given by one of the following two formulae depending on whether the function F involves the parameter φ:

$$\frac{\mathrm{d}J_p}{\mathrm{d}\varphi} = bp\int_\Omega w|F(U,\varphi)-V|^{p-2}[F(U,\varphi)-V]\,\frac{\partial F}{\partial U}s\,\mathrm{d}t \quad \text{if } \frac{\partial F}{\partial\varphi} = 0 \tag{16a}$$

$$\frac{\mathrm{d}J_p}{\mathrm{d}\varphi} = bp\int_\Omega w|F(U,\varphi)-V|^{p-2}[F(U,\varphi)-V]\left(\frac{\partial F}{\partial U}s + \frac{\partial F}{\partial\varphi}\right)\mathrm{d}t \quad \text{if } \frac{\partial F}{\partial\varphi} \neq 0 \tag{16b}$$

Since the sign of s is constant (see Section 3.1) and F is assumed to be monotone, the product $\partial F/\partial U\, s$ keeps the same sign over Ω. Two possibilities arise:

- F is not a function of φ. In this case, Eq. (16a) is applicable. The terms $|F(U,\varphi)-V|^{p-2}$ and $\partial F/\partial U\, s$ in the integral keep a constant sign over Ω, while the second term $F(U) - V$ may change sign. There is a possibility for $\partial J_p/\partial\varphi$ to cancel, which is a desirable property because the purpose of the calibration exercise is to find an optimum of the function J_p.
- F is a function of both U and φ. Then, Eq. (16b) is applicable. In the case of conceptual models (see Section 4), the sign of $\partial F/\partial U s + \partial F/\partial\varphi$ is not necessarily constant because $\partial F/\partial U s$ and $\partial F/\partial\varphi$ may have opposite signs. Then both $[F(U,\varphi)-V]$ and $\partial F/\partial U s + \partial F/\partial\varphi$ in the integral may change sign. In the general case, the two terms do not cancel for the same value of φ, thus increasing the possibilities for the appearance of local extrema.

In both cases, using a strictly positive weighting function w minimizes the number of extrema for J_p.

3.3. Weak form-based objective function

Consider a weak form-based objective function defined from Eq. (7):

$$J_p = a + b\int_\Omega w|F(U,\varphi)-V|^{p-1}[F(U,\varphi)-V]\mathrm{d}t \tag{17}$$

with the same assumptions on F, U and w as in Section 3.2. Then

$$\frac{\mathrm{d}J_p}{\mathrm{d}\varphi} = bp\int_\Omega w|F(U,\varphi)-V|^{p-1}\frac{\partial F}{\partial U}s\,\mathrm{d}t \quad \text{if } \frac{\partial F}{\partial\varphi} \neq 0 \tag{18a}$$

$$\frac{\mathrm{d}J_p}{\mathrm{d}\varphi} = bp\int_\Omega w|F(U,\varphi)-V|^{p-1}\left(\frac{\partial F}{\partial U}s + \frac{\partial F}{\partial\varphi}\right)\mathrm{d}t \quad \text{if } \frac{\partial F}{\partial\varphi} \neq 0 \tag{18b}$$

As in Section 3.2, two possibilities arise:

- F is not a function of the parameter to be calibrated φ. In this case, $\partial F/\partial\varphi = 0$ and Eq. (18a) is applicable. Since $\partial F/\partial U s$ keeps the same sign over Ω the sign of $\partial J_p/\partial x$ cannot change. No local extremum can appear in the objective function.
- F is a function of both U and φ. Then Eq. (18b) applies. The sign of $\partial F/\partial U s + \partial F/\partial\varphi$ is not necessarily constant, as shown in Section 4. This may lead to local extrema in J_p. Nevertheless, the

derivative of J_p as defined by Eq. (18b) is less prone to sign change than that defined in Eq. (16b) because the term $w|F(U,j) - v|^{p-1}$ keeps a constant sign.

3.4. Choice of calibration variables

In the light of the expressions derived in Sections 3.2 and 3.3, the following remarks may be made:

(R9) When calibrating a given model parameter, it is not advised to use a variable, the calculation of which involves this parameter. For instance, in a linear conceptual model, the output discharge is defined as kU, where U is the water level in the reservoir and k is the discharge coefficient. Using U as a calibration variable for k is advisable, while using the discharge kU to calibrate k may generate local extrema in the objective function. Conversely, the discharge kU may be used to calibrate the effective catchment area.

(R10) In many situations however, the only variable available for measurement is not U but a function of U (for instance, the outflowing discharge). In conceptual models, the internal, state variable U of the model is almost never used in calibration/validation procedures, while the discharge, that is only a function of U, is used in almost all situations. Then using a weak form-based objective function minimizes the probability of finding local extrema compared to a distance-based objective function. Consequently, classical gradient-based methods may be used with a larger probability of success to find the zero of the weak form-based objective function than in finding the global optimum of a distance-based objective function.

(R11) Owing to the presence of $\partial F/\partial U$ and $\partial F/\partial \varphi$ in Eqs. (16b) and (18b), using such a function F in the objective function, rather than the primary model variable U, has a strong influence on the direction of the gradient of the objective function in the parameter space. Using several variables of different natures (or transformations of the measured variables), such as water levels and discharges, to calibrate the models, may be more beneficial and more helpful in removing indeterminacy than using several objective functions on the same variables. This was already stated in Beven (2006) about the ill-posed character of the calibration exercise.

(R12) Models with several reservoirs in series have a similar behaviour with respect to the objective function. Indeed, when a reservoir discharges into another, its outflow discharge $g(U,\varphi)$ is the recharge $R(U,t,\varphi)$ of this second reservoir and Assumptions (A1–A4) still hold. Remarks (R9) and (R10) also hold for the calibration of parameters governing the internal fluxes between several reservoirs in a model.

3.5. Objective functions as indicators of parameter redundancy

Assume that two parameters φ_1 and φ_2 in the model are redundant. In this case, for any given variation in φ_1, at least one alternative value can be found for φ_2 such that the modelling result remains unchanged. In other words, in the parameter subspace $\varphi_1 \times \varphi_2$, there exists a relationship in the form

$$\mathrm{d}[F(U)] = 0 \tag{19}$$

Eq. (19) becomes

$$\frac{\partial F(U)}{\partial \varphi_1}\mathrm{d}\varphi_1 + \frac{\partial F(U)}{\partial \varphi_2}\mathrm{d}\varphi_2 = 0 \quad \forall t \tag{20}$$

Eq. (20) defines a hypersurface in the parameter space and a curve in the subspace $\varphi_1 \times \varphi_2$. On the hypersurface (20) one has

$$\mathrm{d}J_p = \frac{\partial J_p}{\partial F(U)}\mathrm{d}[F(U)] = 0 \quad \forall p \tag{21}$$

which means that the objective function is constant along (20). Consequently, the contour lines of the distance-based objective functions (15) obtained with different values of p never intersect. The remark also holds for weak form-based objective functions (17).

An easy way of detecting the redundancy in two model parameters is to plot the contour lines in the subspace $\varphi_1 \times \varphi_2$ of two objective functions (15) or (17) defined with two significantly different values of p (for instance, $p = 1/2$ and $p = 2$). If the contour lines of these two objective functions do not intersect, then the parameters can be suspected to be redundant.

Plotting the contour lines of the objective function requires a systematic exploration of the parameter subspace. An alternative to this approach consists in computing the dimensionless gradients of the objective functions obtained with two different powers p and q:

$$\mathbf{G}_p = \begin{bmatrix} L_1 \frac{\partial J_p}{\partial \varphi_1} \\ L_2 \frac{\partial J_p}{\partial \varphi_2} \end{bmatrix}, \quad \mathbf{G}_q = \begin{bmatrix} L_1 \frac{\partial J_q}{\partial \varphi_1} \\ L_2 \frac{\partial J_q}{\partial \varphi_2} \end{bmatrix} \tag{22}$$

where L_1 and L_2 are scaling factors for the parameters φ_1 and φ_2 (e.g. the typical ranges of variation of these parameters), and checking colinearity via the determinant

$$D = \frac{L_1 L_2}{\|\mathbf{G}_p\|\|\mathbf{G}_q\|}\left(\frac{\partial J_p}{\partial \phi_1}\frac{\partial J_q}{\partial \phi_2} - \frac{\partial J_p}{\partial \phi_2}\frac{\partial J_q}{\partial \phi_1}\right) \tag{23}$$

where the operator $\|\|$ denotes the norm of the vector. The derivatives of the objective functions with respect to the parameters may be computed empirically from two values of J_p and J_q computed using two slightly different values of the parameters. The closer D to zero, the smaller the angle between the gradient vectors G_p and G_q, the more (locally) redundant the parameters φ_1 and φ_2.

4. Application example 1: linear single reservoir model

4.1. Governing equations

Consider a single reservoir, rainfall–runoff model with a linear discharge law:

$$\frac{\mathrm{d}U}{\mathrm{d}t} = AP(t)c - kU \tag{24a}$$

$$U(t_1) = U_1 \geqslant 0 \tag{24b}$$

where A is the catchment area, c is the effective infiltration coefficient, k is the specific discharge coefficient, $P(t)$ is the precipitation rate, U is the volume of water stored in the model and kU is the outlet discharge of the model. Note that Eq. (24a) can be written in the form (8) by defining $g(U,\varphi) = kU$. Classically, A is known and c and/or k must be calibrated.

This model verifies Eqs. (9)–(11) of assumptions (A1)–(A4), consequently $U(t)$ is positive for all t.

The governing equation for the sensitivity is

$$\frac{\mathrm{d}s}{\mathrm{d}t} = -ks - \frac{\partial(kU)}{\partial\varphi} + \frac{\partial(AcP)}{\partial\varphi} \tag{25a}$$

$$s(t_1) = 0 \tag{25b}$$

Two possibilities arise:

(1) The parameter to be calibrated is the effective infiltration coefficient c. In this case, $\varphi = c$ and Eq. (25a) simplifies into

$$\frac{\mathrm{d}s}{\mathrm{d}t} = AP - ks \quad \text{if } \varphi = c \tag{26}$$

Eqs. (25) and (26) verify Eqs. (9)–(12) with $AP > 0$, therefore s is positive for all times.

(1) The parameter to be calibrated is the discharge coefficient k. In this case, $\varphi = k$ and Eq. (25a) becomes

$$\frac{ds}{dt} = -U - ks \quad \text{if } \varphi = k \tag{27}$$

Eqs. (25) and (27) verify Eqs. (9)–(12) with $-U < 0$, therefore s is negative for all times.

4.2. Distance-based objective functions

Assume that a distance-based measure is used for the objective function. If the model is to be calibrated against field measurements (or estimates) of the volume U of water stored in the catchment, then $F(U) = U$ and Eq. (16a) becomes

$$\frac{dJ_p}{d\varphi} = bp \int_\Omega w|U - V|^{p-2}(U - V)s \, dt \tag{28}$$

As shown in the previous subsection, the sign of s is constant over Ω. The particular case of the NSE or SE objective functions, ($p = 2$, $w = 1$) yields the following formula

$$\frac{dJ_2}{d\varphi} = 2b \int_\Omega (U - V)s \, dt \tag{29}$$

Assume now that the model is to be calibrated against the discharge $Q = kU$ at the outlet of the catchment. Then $F(U) = kU$ and $\partial F/\partial U = k$. If the parameter to be calibrated is the coefficient c, then $\varphi = c$ and $\partial F/\partial \varphi = 0$. If the parameter to be calibrated is the discharge coefficient k, then $\varphi = k$ and $\partial F/\partial \varphi = U = Q/k$. Applying Eq. (16) yields

$$\frac{dJ_p}{d\varphi} = bp \int_\Omega w|Q - V|^{p-2}(Q - V)ks \, dt \quad \text{if } \varphi = c \tag{30a}$$

$$\begin{aligned}\frac{dJ_p}{d\varphi} &= bp \int_\Omega w|Q - V|^{p-2}(Q - V)(ks + Q/k) \, dt \\ &= -bp \int_\Omega w|Q - V|^{p-2}(Q - V)\frac{ds}{dt} \, dt \quad \text{if } \varphi = k\end{aligned} \tag{30b}$$

Note that the second equality in Eq. (30b) is obtained from Eq. (27). Since s is not monotone over Ω in the general case, both $Q - V$ and ds/dt are liable to cancel over Ω and the objective function J_p in Eq. (30b) may have more than one extremum. This is an illustration of Remark (R10). In the particular case of the NSE or SE objective functions ($p = 2$, $w = 1$), the following formulae are obtained

$$\frac{dJ_2}{d\varphi} = 2b \int_\Omega (Q - V)ks \, dt \quad \text{if } \varphi = c \tag{31a}$$

$$\begin{aligned}\frac{dJ_2}{d\varphi} &= 2b \int_\Omega (Q - V)(ks + Q/k) dt \\ &= -2b \int_\Omega (Q - V)\frac{ds}{dt} \, dt \quad \text{if } \varphi = k\end{aligned} \tag{31b}$$

4.3. Weak form-based objective function

Assume now that the objective function is defined using the weak form-based approach.

If the model is to be calibrated against field measurements (or estimates) of the volume of water stored in the catchment, then $F(U) = U$ and Eq. (18) becomes

$$\frac{dJ_p}{d\varphi} = bp \int_\Omega w|U - V|^p s \, dt \tag{32}$$

Since s keeps the same sign over Ω the derivative of J_p cannot cancel if w is nonzero. Then the points for which $J_p = a$ (a being the optimum value for the objective function) define a line in the parameter space (c, k). In the particular case ($p = 2$, $w = 1$), one has

$$\frac{dJ_2}{d\varphi} = 2b \int_\Omega (U - V)^2 s \, dt \tag{33}$$

If the model is to be calibrated using measurements of the outlet discharge $Q = kU$, then $F = kU$, $\partial F/\partial U = k$ and Eq. (18) gives

$$\frac{dJ_p}{d\varphi} = bp \int_\Omega w|Q - V|^{p-1}ks \, dt \quad \text{if } \varphi = c \tag{34a}$$

$$\begin{aligned}\frac{dJ_p}{d\varphi} &= bp \int_\Omega w|Q - V|^{p-1}(ks + Q/k)dt \\ &= -bp \int_\Omega w|Q - V|^{p-1}\frac{ds}{dt} \, dt \quad \text{if } \varphi = k\end{aligned} \tag{34b}$$

An interesting, particular case is that of the Cumulative Error (CE), or Balance Error (BE) indicators (see Appendix A), obtained for ($p = 1$, $w = 1$):

$$\frac{dJ_p}{d\varphi} = bA \int_\Omega ks \, dt = bAk \int_\Omega s \, dt \quad \text{if } \varphi = c \tag{35a}$$

$$\frac{dJ_p}{d\varphi} = -b \int_\Omega \frac{ds}{dt} \, dt = -b[s(t_2) - s(t_1)] \quad \text{if } \varphi = k \tag{35b}$$

Two remarks may be made:

(R13) It is visible from Eq. (32) that the derivative of the weak form-based objective function cannot be zero, except in the trivial case ($U = V \; \forall \, t \in \Omega$). If the objective function is based on the outlet discharge $Q = kU$ (Eq. (34)), the only possibility for its derivative to cancel in the non-trivial case ($Q = V \; \forall \, t \in \Omega$) occurs for $k = 0$, which is meaningful only in the trivial case $kU = V = 0 \; \forall \, t \in \Omega$.

(R14) Comparing Eqs. (35a) and (35b) indicates that the CE and BE indicators are extremely useful in calibrating the runoff coefficient c but are almost useless in calibrating the discharge coefficient k of the conceptual model. This well-known result is confirmed by the following analysis. The ratio of the gradients computed via Eqs. (35a) and (35b) gives

$$\frac{dJ_p}{dk} = K\frac{dJ_p}{dc} \tag{36a}$$

$$K = \frac{s(t_2) - s(t_1)}{k\int_\Omega s \, dt} = \frac{s(t_2) - s(t_1)}{(t_2 - t_1)k\bar{s}} \tag{36b}$$

where $\bar{s}$ is the average value of s over Ω. The numerator in K remains bounded. If the input time series is sufficiently long to be assumed stationary, the average value of s does not depend on the length of the time interval $t_2 - t_1$. Consequently the denominator is proportional to the time interval $t_2 - t_1$. Therefore K tends to zero as the length of the calibration interval increases. This means that the CE and BE indicators are insensitive to the value of k when long time series are used. Therefore, they cannot be used to calibrate k when the variable is the outflowing discharge.

4.4. Numerical experiments

The properties of distance- and weak form-based objective functions are investigated using the following numerical experiment. An artificial time series for the observed (measured) variable V is generated using a nonlinear conceptual model with artificially randomized input time series. The water level in the nonlinear

reservoir and the outflowing discharge of the nonlinear model are considered as «reality», against which a linear conceptual model is to be fitted. The steps in the generation of the times series are the following.

(1) An artificial rainfall time series is generated at a daily time step using the following model:

$$P_n = \frac{P_{\max}}{1-\alpha}\max(\mathrm{Ran}-\alpha,0) \tag{37}$$

where $P_{\max}$ is a constant, Ran is generated randomly from a uniform probability density function between 0 and 1, and α is a threshold value between 0 and 1. Ran is generated every time step independently from the realization at the previous time steps. The probability for a rainfall R_n to be nonzero over a given day n is $1-\alpha$.

(1) The generated rainfall signal is used as an input for a nonlinear conceptual model obeying the following equation:

$$\frac{\mathrm{d}W}{\mathrm{d}t} = A(CP - KW^{\beta}) \tag{38a}$$

$$W(0) = 0 \tag{38b}$$

where A is the catchment area, C is an infiltration constant, K and β are predefined constants ($\beta \neq 1$) and W is the amount of water stored in the model. Eq. (38a) is solved numerically using an explicit formula at a daily time step:

$$W_{n+1} = W_n + A(CP_n - KW_n^{\beta})\Delta t \tag{39}$$

where P_n is the average value of the rainfall rate between the time levels n and $n+1$. The explicit approach corresponds to the most widespread implementation of conceptual models available in the literature.

(1) The numerical solution W_n is used as the observed variable V in the computation of the objective function. Two possibilities are considered hereafter:

$$\left.\begin{aligned} V &= W \\ F(U) &= U \end{aligned}\right\} \tag{40a}$$

$$\left.\begin{aligned} V &= AKW^{\beta} \\ F(U) &= AkU \end{aligned}\right\} \tag{40b}$$

Eq. (40a) corresponds to the situation where the state variable W can be field-estimated or measured and where the variable U in the linear model (24a) is considered to bear a physical meaning. Eq. (40b) correspond to the more widespread calibration technique where the variable used in the computation of the objective function is the discharge at the outlet of the catchment.

Note that the governing Eq. (24a) for the linear reservoir model is also solved numerically using an explicit formula

$$U_{n+1} = U_n + A(cP_n - kU_n)\Delta t \tag{41}$$

where c and k are the infiltration coefficient and the specific discharge coefficient for the linear conceptual model. The main motivation behind the choice of a nonlinear conceptual model to generate the reference time series is that no combination of the parameters c and k in the linear model (24a) allows the solution W of Eq. (38a) to be reproduced exactly, which is precisely the case when real-world time series are dealt with.

The parameters used in the present experiment are summarized in Table 1.

Fig. 1 shows the contour lines obtained for two types of distance-based objective functions. The first objective function $J_{p,U}$ is defined using the amount of water in the reservoir as in Eq. (40a):

Table 1
Linear reservoir model. Parameters for the numerical experiment.

Symbol	Meaning	Value
A	Catchment area	200 km^2
C	Infiltration coefficient in the nonlinear model	0.5
K	Discharge coefficient in the nonlinear model	10^{-11} m$^{-(1-3\beta)}$ day^{-1}
$P_{\max}$	Maximum rainfall rate	60 mm day^{-1}
T	Length of the simulation	10^4 days
α	Threshold for rainfall generation	0.9
β	Exponent in the nonlinear rainfall–runoff model	2.0
Δt	Computational time step	1 day

$$J_{p,U} = 1 - \frac{\int_\Omega |U-W|^p \,\mathrm{d}t}{\int_\Omega |\overline{W}-W|^p \,\mathrm{d}t} \tag{42}$$

The second objective function $J_{p,Q}$ is computed from the outflow discharges as in Eq. (40b):

$$J_{p,Q} = 1 - \frac{\int_\Omega |Q-KW^{\beta}|^p \,\mathrm{d}t}{\int_\Omega |\overline{KW^{\beta}}-KW^{\beta}|^p \,\mathrm{d}t} \tag{43}$$

where the overbar denotes the average over Ω. Eqs. (42) and (43) are nothing but the Generalized Nash–Sutcliffe Efficiency (GNSE) presented in Appendix A. In hydrological modelling, it is more customary to use the discharge as a calibration variable than the volumes stored in the reservoirs. In Fig. 1, the values used for p are 1/2, 1 and 2.

Comparing the contour lines obtained using Eq. (42) (Fig. 1a, c, and e) and those obtained using Eq. (43) (Fig. 1b, d, and f) illustrates Remark (R11). The objective functions based on the water depth (or volume) and the objective functions based on the discharge have radically different contour line shapes. Using two different variables in the definition of the objective functions brings in more information than using the same variables and changing the value of the power p in the GNSE. Obviously, the optimal parameters for the objective functions depend on the variable used in the calibration process and, to a lesser extent, on the value of the exponent p. The discharge MSE grows by a factor four when switching the calibration variable from discharge Q to the internal variable U, using the MSE objective function.

Remarks (R9, R10) are illustrated by the zero contour line in Fig. 1d. It is visible from Fig. 1d that the derivative $\partial J_{1/2,Q}/\partial k$ cancels for small values of k around $c = 1.0$. This corresponds to the change in curvature of the zero contour line next to the c-axis. The objective function is not monotone with respect to k in this region of the parameter space. In the present case, however, this is not too serious a problem because (i) the extremum corresponds to a minimum in the objective function, and (ii) it is located far away from the maximum of the objective function. However, in the general case, this is a potential source for local extrema in the objective function.

Fig. 2 shows the contour lines obtained for two types of weak form-based objective functions. The first objective function $J_{p,U}$ is defined using the state variables U and W as in Eq. (40a):

$$J_{p,U} = \frac{\int_\Omega |U-W|^{p-1}(U-W)\mathrm{d}t}{\int_\Omega |\overline{W}-W|^p \,\mathrm{d}t} \tag{44}$$

The second objective function $J_{p,Q}$ is computed from the outflow discharges as in Eq. (40b):

$$J_{p,Q} = \frac{\int_\Omega |Q-KW^{\beta}|^{p-1}(Q-KW^{\beta})\mathrm{d}t}{\int_\Omega |\overline{KW^{\beta}}-KW^{\beta}|^p \,\mathrm{d}t} \tag{45}$$

where the overbar denotes the average over Ω. Note that the denominator in Eqs. (44) and (45) is similar to that in Eqs. (42)

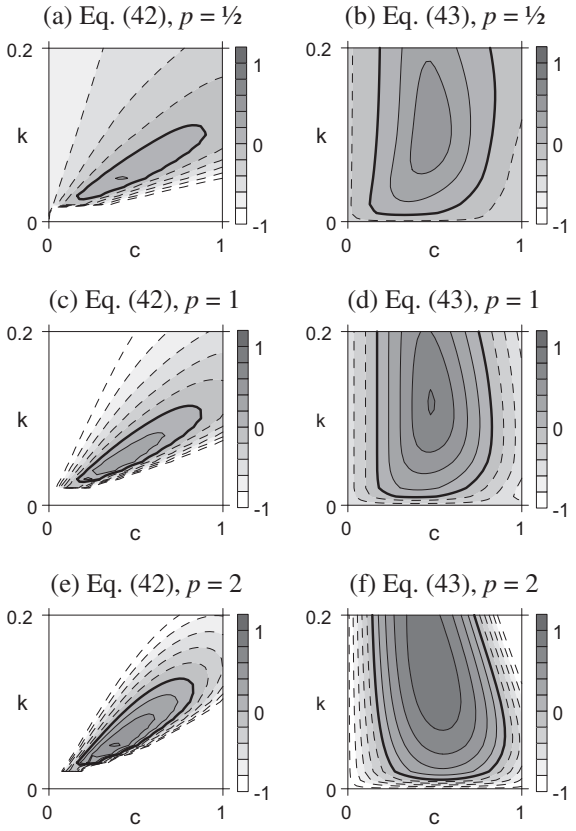

Fig. 1. Linear reservoir model. Contour lines for the distance-based objective functions. Left: using measured storage W, Eq. (42); right: using measured outflow, Eq. (43). Contour line spacing 0.2. Dashed lines: negative values; solid lines: positive values; bold line: zero contour line. Optimum parameter values are those for which the objective function is maximum.

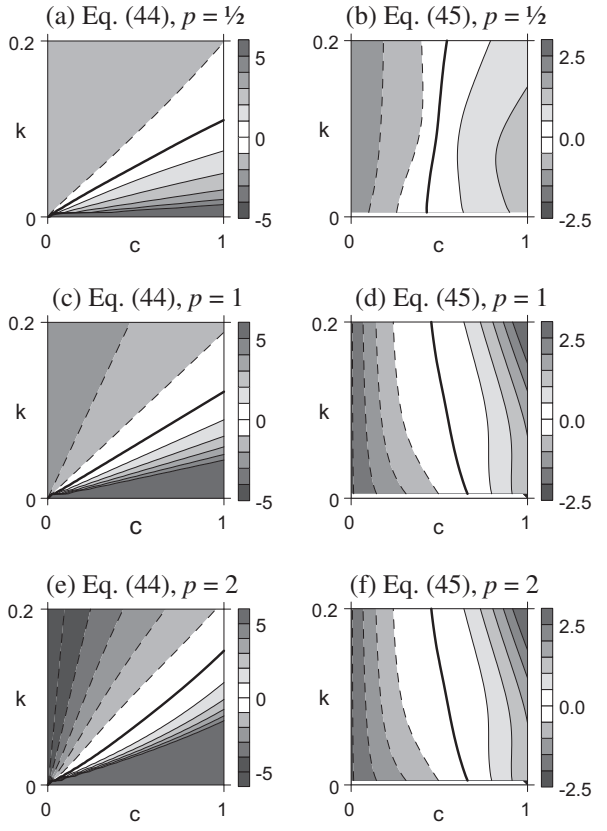

Fig. 2. Linear reservoir model. Contour lines for the weak form-based objective functions. Left: using measured storage W, Eq. (44); right: using measured outflow, Eq. (45). Dashed lines: negative values; solid lines: positive values; bold line: zero contour. Optimum parameter values are those for which the objective function is zero.

and (43) and therefore the scaling is the same. In contrast with Eqs. (42) and (43), the best model fit is achieved for $J_{p,U} = 0$ and $J_{p,Q} = 0$. Also note that for $p = 1$ (Fig. 2d), Eq. (45) gives an information similar to the Cumulative Error (CE) or Balance Error (BE).

Remarks (R9, R10) are illustrated by the zero contour line in Fig. 2b. Indeed, the derivative $\partial J_{1/2,Q}/\partial k$ cancels for ($k = 0.15$, $c = 0.2$). This corresponds to the curved contour in the bottom right corner of the Figure. The objective function is not monotone with respect to k in this region of the parameter space.

As in the case of the distance-based objective functions (42) and (43), comparing Fig. 2a–f illustrates Remark (R11) on the complementary character of the information brought by objective functions defined using different model variables. However, contrary to distance-based objective functions, it is possible to find parameter combinations for which the objective functions defined by both Eqs. (44) and (45) are optimal.

Remark (R13) on the strictly monotone character of the weak form-based objective functions is also confirmed.

Fig. 2d confirms Remark (R14) that the specific discharge coefficient k cannot be calibrated using CE or BE because the CE and BE indicators have identical values for all k. At the same time, the CE or BE indicators are extremely useful in calibrating the infiltration coefficient because there is only one possible value of c for which $J_{1,Q} = 0$.

Moreover, the intersection of all the zero contour lines in Fig. 2 are very close to the optimum values for the distance-based objective functions using the discharge as a calibration variable (Fig. 1b, d, and f). This indicates that the set of weak form-based objective functions may yield a calibration result close to that given by the commonly admitted distance-based approach, while eliminating the local extremum problem associated with distance-based objective functions.

This example also illustrates the fact that optimum values obtained from distance-based functions are often mutually exclusive – a parameter set optimal for one criterion may be far from satisfactory for another criterion –, which is not the case with weak form-based functions.

5. Application example 2: a multiple reservoir model with threshold function

The purpose of this example is to illustrate application of the proposed redundancy test.

5.1. Model presentation

The Medor model (Hreiche et al., 2003) is a three-reservoir model (Fig. 3) initially designed for hydrological modelling over arid or semi-arid regions. A variation of this model has been applied recently to the modelling of karst catchments in the Mediterranean area (Fleury, 2005; Tritz et al., 2011). The top reservoir accounts for production. The input to this reservoir is the precipitation rate P, the outputs are the evapotranspiration rate E and the net precipitation rate I. E may be set equal to the potential rate, computed from standard evapotranspiration formulae (Fleury, 2005), or interpolated from monthly data (Tritz et al., 2011). E is limited only when the reservoir is empty ($H = 0$) and precipitation are insufficient ($P < E$). I is zero until the water level H in the production reservoir reaches the maximum value H_{max}. In such a case, the net input $P - E$ is transferred instantaneously to the other two

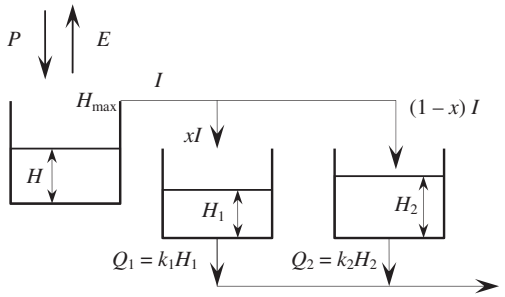

Fig. 3. Medor model. Structure, flow chart and notation.

reservoirs. From a conceptual point of view, the production reservoir represents the soil layer, from which previously precipitated water may be restituted to the atmosphere via evapotranspiration. Note that when the soil reservoir is empty, it remains so until $P - E$ becomes positive again.

The net precipitation is routed to a fast response and a slow response reservoir via a distribution coefficient x, $0(x \leqslant 1$. Each of these two reservoirs obeys a linear discharge law. The output hydrograph is the sum of the output discharges from the fast and slow reservoir. From a physical point of view, the two reservoirs may account for different flow routing paths over the catchment. From the point of view of the transfer function of the model, such a structure allows both the rapid recession part of hydrographs and the slower fluctuations of the base flow to be accounted for via linear laws.

The governing balance equations are the following:

$$\frac{dH}{dt} = \begin{cases} P - E - I & \text{if } H > 0 \\ 0 & \text{if } H = 0 \text{ and } P - E < 0 \end{cases} \tag{46a}$$

$$\frac{dH_1}{dt} = xI - \frac{Q_1}{A} \tag{46b}$$

$$\frac{dH_2}{dt} = (1 - x)I - \frac{Q_2}{A} \tag{46c}$$

where H_1 and H_2 are respectively the water levels in the fast and slow reservoirs. I, Q_1 and Q_2 are given by

$$I = \begin{cases} 0 & \text{if } H < H_{max} \\ P - E & \text{if } H = H_{max} \end{cases} \tag{47a}$$

$$Q_1 = Ak_1H_1 \tag{47b}$$

$$Q_2 = Ak_2H_2 \tag{47c}$$

where k_1 and k_2 are the specific discharge coefficients of the two reservoirs. The total outflowing discharge is computed as the sum of Q_1 and Q_2.

5.2. Principle of the parameter redundancy test

It is first noticed that the total amount of water flowing to the outlets of the reservoirs is strongly conditioned by the maximum water level H_{max} in the production reservoir. Indeed, I is nonzero only when H reaches H_{max}. The larger H_{max}, the smaller the time during which I is nonzero, the smaller the amount of water flowing to the reservoirs H_1 and H_2.

Consider now the configuration of the model where the specific discharge coefficient of one of the two reservoirs (say, k_2) is zero. In this case, the water may accumulate indefinitely in this reservoir, while the outflowing discharge from this reservoir remains zero. In other words, if $k_2 = 0$, the reservoir H_2 acts as a loss and only a fraction xI of the total infiltration rates participates to the outflow. Therefore, x also controls the outflowing discharge to some extent.

Clearly, H_{max} and x exert a similar influence on the outflowing discharge when $k_2 = 0$. In other words, they are redundant with respect to total discharge, for $k_2 = 0$. Consequently, plotting two different objective functions (18a) and (18b) with two different values of p in the parameter space (H_{max}, x) should yield non-intersecting contour lines for the two objective functions.

5.3. Catchment and modelling data

The Medor model was used to simulate daily discharge at the outlet of the Bani catchment (Fig. 4). This large west-African catchment is characterized by a monsoon climate with a strong north–south rainfall gradient, and considerable rainfall variability since the mid-20th century. As a result, the flow at the Douna gauging station (Fig. 4) fell by 68% from 1952–1970 to 1971–2000, with a decrease in the deep water recharge and in base runoff contribution to the annual flood (Ruelland et al., 2009). Some of the low-water periods were severe to the point that river flow at Douna stopped at times during the 1980s.

The Medor model may seem too simple at first sight for an operation at a daily time step given the dimensions of the catchment and the time scale of the discharge signal. However, experiments carried out using models of varying complexity have shown that complex transfer functions involving signal delay (such as the unit hydrograph convolution approach) do not contribute to improve model performance significantly (Ruelland et al., 2010). In a similar fashion, using spatially distributed rainfall inputs and model parameters was not seen to improve the quality of the simulated hydrographs significantly. The inertia of the linear reservoirs in the Medor model are seen to be sufficient to model the rainfall-discharge transformation in a satisfactory way. This simpler model is thus retained for the analysis.

The model was applied to the 1967–1985 period, for which the discharge record was continuous at the Douna station. Daily rain series were derived from 72 rain gauges covering the area (Fig. 4). An average of 70 gauges (with a minimum of 66) were used to interpolate daily rainfall maps by the inverse distance method, which proved to perform best (Ruelland et al., 2008). Potential evapotranspiration forcing consisted of monthly maps produced by the Climatic Research Unit (University of East Anglia, UK) from ~100 stations spread over West Africa, using Penman's method and spline interpolation (New et al., 2000). Since potential evapotranspiration varies slowly over the year, monthly data were disaggregated evenly to the daily time step within each month. The first five years of simulation were used as model warm-up, to eliminate the influence of initial conditions. This five year period was determined from the order of magnitude of the specific discharge coefficients in the model (from 2.5×10^{-3} to 2×10^{-1}). Indeed, as shown in Section B.3, a model with a specific discharge coefficient k requires a warm-up period of at least a few times $1/k$ for the influence of initial conditions to be eliminated. The parameters used in the experiment are given in Table 2. The catchment area A is known from previous studies (Ruelland et al., 2008), while the specific discharge coefficient k_1 is taken equal to the value that allows the NSE index to be maximized.

5.4. Redundancy test results

Fig. 5 shows, in the (H_{max}, x) space, the contour lines obtained for the distance-based and weak form-based objective functions computed from the discharge observations. The powers used in Eqs. (43) and (45) are $p = 1/2$ and $p = 2$.

Fig. 5e is a superimposition of Fig. 5a and c, while Fig. 5f results from the superimposition of Fig. 5b and d. In Fig. 5e–f, the dashed

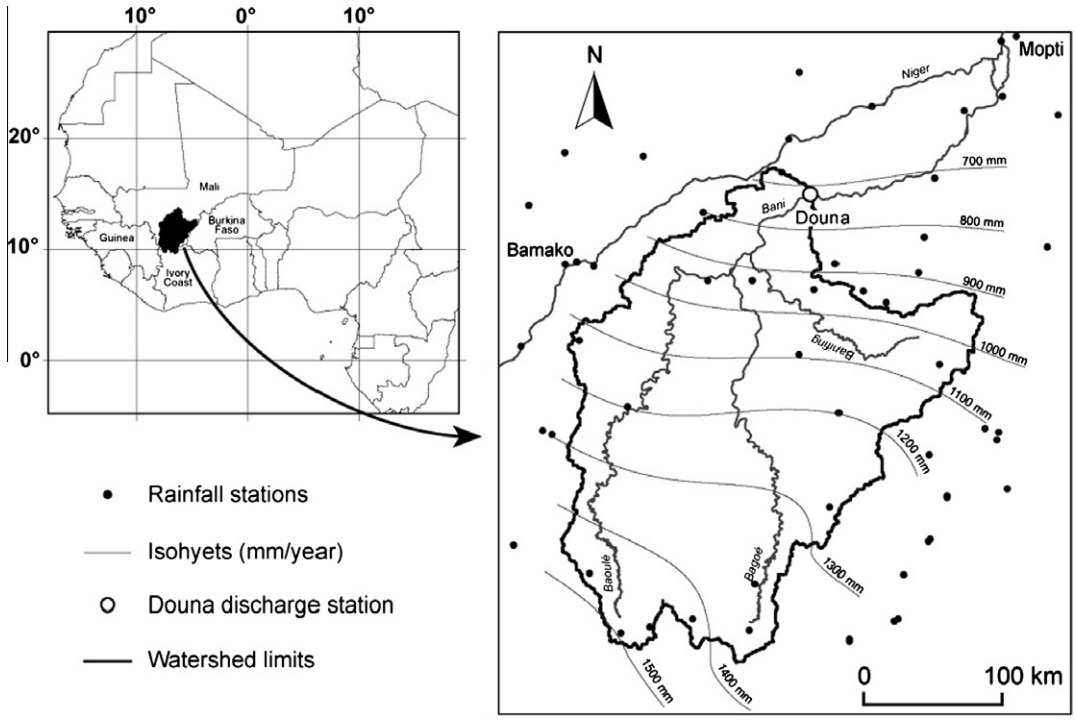

Fig. 4. The Bani catchment at Douna: rainfall and discharge stations used.

Table 2
Multiple reservoir model. Parameters for the redundancy test.

Symbol	Meaning	Value
A	Catchment area	104,000 km^2
H_{max}	Maximum depth in the soil reservoir	0 – 1 m
k_1	Specific discharge coefficient for reservoir 1	5×10^{-2} day^{-1}
k_2	Specific discharge coefficient for reservoir 2	0 day^{-1}
T	Length of the simulation	6935 days
x	Reservoir distribution coefficient	0 – 1
Δt	Computational time step	1 day

and solid lines are respectively the contour lines of the objective functions for $p = 1/2$ and $p = 2$. Except in the upper left part of the diagram, the contour lines do not intersect, which confirms that the parameters H_{max} and x become redundant over most of the parameter space when $k_1 = 0$ or $k_2 = 0$.

6. Conclusions

Model performance assessment and objective functions classically used in hydrological modelling may be classified into distance-based and weak form-based objective functions.

Distance-based objective functions have the advantage that the calibration problem is transformed into a straightforward, single-criterion optimization problem. Their drawback is the possible appearance of local extrema in the response surface of the model, thus triggering the failure of classical gradient-based methods and requiring the use of more computationally demanding global optimization algorithms.

Weak form-based objective functions transform the calibration exercise into a root finding problem.

The theoretical considerations in Sections 2–3 and the application examples in Sections 4–5 lead to the following conclusions.

(C1) Weak form-based objective functions are more monotone than distance-based objective functions when applied to

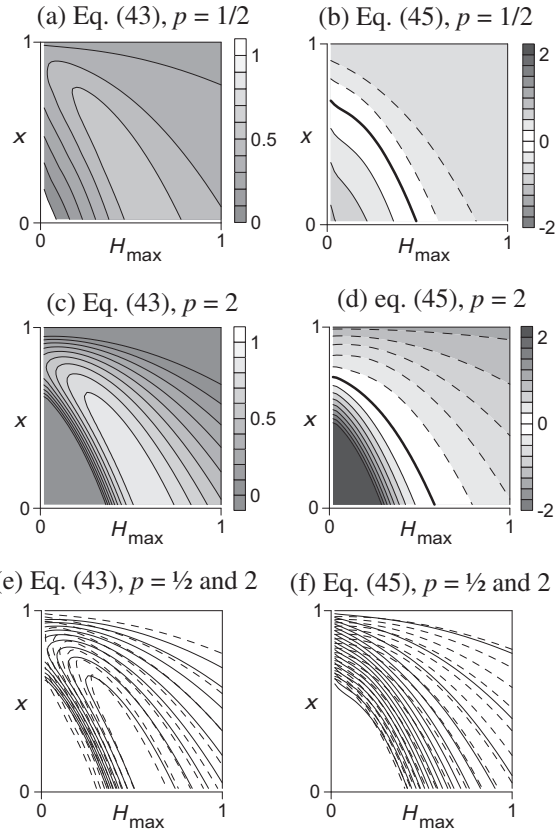

Fig. 5. Multiple reservoir model. Contour lines for the objective functions. Left: distance-based function, Eq. (43); right: weak form-based function, Eq. (45). Dashed lines: negative values; solid lines: positive values; bold line: zero value. Optimum parameter values are those for which the objective function in (b), (d) is zero. (e and f): Dashed line: $p = 1/2$; bold line: $p = 2$.

conceptual hydrological models. Monotony can be proved mathematically for models verifying Assumptions (A1–A4) in Section 3.1.

(C2) The subset of zero values of weak form-based objective functions form hypersurfaces in the parameter space. A model with N parameters can be calibrated by defining N weak form-based objective functions and finding the intersection of the corresponding N hypersurfaces in the parameter space. Since the weak form-based objective functions are monotone, the intersection is unique. This allows classical gradient-based algorithms to be used without the need for more sophisticated optimum search techniques. The N different objective functions may be defined by using (i) different observation variables, (ii) transformations of these variables, (iii) different values for the power p used in the formulation of the weak form-based function (see Eq. (7)). Note that the need for a number of independent criteria matching the number of parameters to be calibrated was already pointed out by Gupta et al. (2008).

(C3) In contrast, distance-based objective functions yield mutually exclusive optimal parameter sets when different calibration variables are used. Using weak form-based objective functions allows this drawback to be eliminated. This allows for multi-objective calibration without the inconvenience of multiple solutions.

(C4) Distance-based objective functions being widely recognized in the field of hydrological modelling, they could also be used in combination with weak form-based objective functions in the framework of multi-criteria optimization algorithms. A typical multi-criteria optimization problem may then consist in maximizing the distance-based objective function under the constraint that all the weak form-based objective functions are zero.

(C5) Using the same type of objective function (distance-based, see Eq. (48) or weak form-based, see Eq. (49)) with two different values of p yields two families of contour surfaces in the parameter space. Non-intersecting families of contour surfaces in the parameter space indicate redundancy between two or more parameters.

(C6) The theoretical analysis in Section 3 and the application example in Section 4 show that using the volume stored in the reservoir as a calibration variable for the discharge coefficient may be more appropriate than using the discharge. Conversely, the outlet discharge may be a more appropriate variable to calibrate an infiltration (or net rainfall) coefficient via a weak form-based objective function.

(C7) Assuming that weak form-based objective functions are to be used, the calibration problem is best posed when the hypersurfaces as defined in (C2) are as orthogonal to each other as possible. Therefore, it is advisable to define such objective functions using as many different model state variables as possible (e.g. discharges between various reservoirs in the model, volumes stored in the various reservoirs, etc.).

(C8) A necessary condition for (C5 and C6) to be applicable, however, is that the internal variables and fluxes in the model bear a physical reality and be field-measurable. Due to hydrological/hydraulic variability, translating field measurements (e.g. of soil moisture, or piezometric head in aquifers) into variations of model internal variables is not an easy task. This most probably calls for the definition of a different kind of objective functions. For instance, the trends (rising or falling; increasing or decreasing) of the measured and model internal variables over certain periods may be used in the form of indicators. Note that internal variables may be useful even if not incorporated into the objective function: they may be used to discriminate between different models (or different parameter sets within the same model) giving similar values of objective functions computed from the outflowing fluxes. Note that extending the model to water quality variables has been shown to reduce parameter uncertainty (Kuczera and Mroczkowski, 1998).

(C9) The result of the calibration/validation process may be biased if the model has not been run over a sufficiently long warm-up period for the influence of possibly inaccurate initial conditions to be eliminated (see Section B.2 in Appendix B). The minimum length of the warm-up period is a function of the parameters of the model. Consequently, it should not only be defined a priori: an a posteriori check is needed once the model has been calibrated.

The theoretical considerations presented in this paper are valid for hydrological models obeying first-order differential equations. Whether such conclusions also hold for models involving delay functions (e.g. the GR3J model (Edijatno et al., 1999) that embeds a unit hydrograph transformation) or other functions not verifying exactly the governing assumptions in Section 3 is the subject of ongoing research. Future research should also focus on (i) the robustness of weak form-based objective functions compared to the well-established distance-based approach and (ii) the effects of data uncertainty on the behaviour of the objective function. Although only conceptual models were considered in this study, the approach might be applicable to the calibration of some physically-based hydrological models, e.g. when backwater effects are insignificant, however such extrapolation should be subject to further theoretical investigation.

Acknowledgements

This work was supported by an Internal Project financed by the Laboratory HydroSciences Montpellier (HSM, UMR5569, CNRS, IRD, UM1, UM2). The anonymous reviewers are thanked for their constructive comments that helped improve this paper.

Appendix A. Classical objective functions

The functions are classified in Table A.1 into to Distance-based (D) and Weak form-based (W) objective functions. a, b and p in Table A.1 are respectively the offset constant, the scaling constant and the power used in Eqs. (4) and (7).

Appendix B. Proofs

B.1. Sign of the solution U of Eq. (8)

Assume that Eq. (8) holds, with assumptions (A1–A4) verified. From Assumption (A3), at any time t there exists $U_0(t) > 0$ such that $\mathrm{d}U/\mathrm{d}t = 0$ for $U = U_0$. U_0 verifies Eq. (11), that is:

$$g(U_0, \varphi) = R(U_0, \varphi, t) \tag{B.1}$$

If $U(t)$ is smaller than U_0, then $\mathrm{d}U/\mathrm{d}t = R - g$ is positive because of Assumption (A2), and U can only increase at time t. Hence, $U(t)$ is either greater than U_0 or increasing, and thus can never be negative for $t > t_1$ since $U(t_1) \geqslant 0$ (Assumption (A4)).

Table A.1

Name	Reference	Formula	Type	a	b	p
Nash–Sutcliffe efficiency	Nash and Sutcliffe (1970)	$\mathrm{NSE}=1-\frac{\int_\Omega (U-V)^2\mathrm{d}t}{\int_\Omega (\overline{V}-V)^2\mathrm{d}t}$	D	1	$-[\int_\Omega (\overline{V}-V)^2\mathrm{d}t]^{-1}$	2
Square error		$\mathrm{SE}=\int_\Omega (U-V)^2\mathrm{d}t$	D	0	1	2
Root mean square error	Hogue et al. (2000)	$\mathrm{RMSE}=\left[\frac{\int_\Omega (U-V)^2\mathrm{d}t}{\int_\Omega \mathrm{d}t}\right]^{1/2}$	D	0	$[\int_\Omega \mathrm{d}t]^{-1}$	2
Mean absolute error	Perrin et al. (2001)	$\mathrm{MAE}=\frac{\int_\Omega \lvert U-V\rvert \mathrm{d}t}{\int_\Omega \mathrm{d}t}$	D	0	$[\int_\Omega \mathrm{d}t]^{-1}$	1
Volumetric efficiency/bias	Criss and Winston (2008) Hogue et al. (2006)	$\mathrm{VE}=1-\frac{\int_\Omega \lvert U-V\rvert \mathrm{d}t}{\int_\Omega V\ \mathrm{d}t}$	D	1	$-[\int_\Omega V\ \mathrm{d}t]^{-1}$	1
Generalized Nash–Sutcliffe efficiency	Legates and McCabe (1999)	$\mathrm{GNSE}=1-\frac{\int_\Omega \lvert U-V\rvert^p \mathrm{d}t}{\int_\Omega \lvert \overline{V}-V\rvert^p \mathrm{d}t}$	D	1	$-[\int_\Omega \lvert \overline{V}-V\rvert^p \mathrm{d}t]^{-1}$	Any value
Volume error/cumulative error	Madsen (2000)/Perrin et al. (2001)	$\mathrm{CE}=\int_\Omega (V-U)\mathrm{d}t$	W	0	1	1
Balance error	Perrin et al. (2001)	$\mathrm{BE}=\frac{\int_\Omega (V-U)\mathrm{d}t}{\int_\Omega V\ \mathrm{d}t}$	W	0	$[\int_\Omega V\ \mathrm{d}t]^{-1}$	1

B.2. Sign of the sensitivity s in Eq. (13)

The sensitivity Eq. (13) are rewritten as

$$\frac{\mathrm{d}s}{\mathrm{d}t}=\alpha s+\beta \tag{B.2a}$$

$$\alpha=\frac{\partial}{\partial U}(R-g) \tag{B.2b}$$

$$\beta=\frac{\partial}{\partial \varphi}(R-g) \tag{B.2c}$$

$$s(t_1)=0 \tag{B.2d}$$

From assumption (A2), α is negative and β has a constant sign. The case $\beta=0$ leads to the trivial solution $s=0$ and is not considered hereafter.

Consider first the case $\beta>0$. In this case, there exists an equilibrium value $s_0=-\beta/\alpha$ for the sensitivity, with $\mathrm{d}s/\mathrm{d}t=0$ for $s=s_0$ in Eq. (B.2a). Since α is negative and β is positive, s_0 is always positive. If $s<s_0$, $\mathrm{d}s/\mathrm{d}t=\alpha s+\beta>0$. Hence, s is either larger than the positive value s_0 or increasing. Since $s(t_1)=0$ (Eq. (13b)), $\mathrm{d}s/\mathrm{d}t>0$ at $t=t_1$ and $s(t)>0$ for all $t>t_1$.

Reasoning by symmetry leads to the conclusion that $s(t)<0$ for all $t>t_1$ when $\beta<0$.

B.3. Sensitivity to initial conditions and model warm-up period

The purpose is to study the sensitivity of model output to the initial conditions. Consider the linear model where R and g are:

$$R=P-ET \tag{B.3a}$$

$$g=-kU \tag{B.3b}$$

If the purpose is to study the influence of initial conditions, the parameter φ is $\varphi=U_0$. In this case, α and β in Eq. (B.2a) are given by

$$\alpha=-k \tag{B.4a}$$

$$\beta=0 \tag{B.5a}$$

Considering that the sensitivity of U with respect to the initial condition is equal to 1 for $t=0$, the solution of Eqs. (B.2a), (B.4a), and (B.4b) is a decreasing exponential:

$$s(t)=\exp(-kt) \tag{B.6}$$

The sensitivity of U (and therefore of any function $F(U)$) becomes negligible after a simulation period equal to a few times $1/k$. The warm-up period, that is necessary to eliminate the influence of a possible wrongly defined initial condition, should therefore be taken equal to a few times $1/k$. For instance, $s(3/k)=4.98\%$; $s(4/k)=1.8\%$ and $s(5/k)=0.7\%$. In other words, only 0.7% of the initial sensitivity to the initial conditions remains after a simulation period $5/k$.

References

Beven, K., 1993. Prophecy, reality and uncertainty in distributed hydrological modelling. Advances in Water Resources 16, 41–51.

Beven, K., 2006. A manifesto for the equifinality thesis. Journal of Hydrology 320, 18–36.

Beven, K., Binley, A., 1992. The future of distributed models: model calibration and uncertainty prediction. Hydrological Processes 6, 279–298.

Brazil, L.E., Krajewski, W.F., 1987. Optimisation of complex hydrologic simulation models using random search methods. Engineering Hydrology Proceedings, Hydraulics Division/ASCE/Williamsburg, Virginia, August 3–7, 726–731.

Cacuci, D.G., 2003. Sensitivity and Uncertainty Analysis. Theory. Chapman & Hall/CRC, 285p.

Cappelaere, B., Vieux, B., Peugeot, C., Maia-Bresson, A., Séguis, L., 2003. Hydrologic process simulation of a semiarid, endorheic catchment in Sahelian West Niger–2. Model calibration and uncertainty characterization. Journal of Hydrology 279, 244–261.

Courant, R., Hilbert, D., 1953. Methods of Mathematical Physics. Interscience Publishers Inc., New York. 830p.

Criss, R.E., Winston, W.E., 2008. Do Nash values have value? Discussion and alternate proposals. Hydrological Processes 22, 2723–2725.

Duan, Q., Sorooshian, S., Gupta, V.K., 1992. Effective and efficient global optimisation for conceptual rainfall–runoff model. Water Resources Research 28 (4), 1015–1031.

Edijatno, N.N., Yang, X., Makhlouf, Z., Michel, C., 1999. GR3J: a daily watershed model with three free parameters. Hydrological Sciences Journal 44, 263–278.

Efstratiadis, A., Koutsoyiannis, D., 2010. One decade of multi-objective calibration approaches in hydrological modelling: a review. Hydrological Sciences Journal 55 (1), 58–78.

Fleury, P., 2005. Sources sous-marines et aquifères karstiques côtiers méditerranéens. Fonctionnement et caractérisation. Ph.D thesis, University Paris 6 (France).

Freedman, V.L., Lopes, V.L., Hernandez, M., 1998. Parameter identifiability for catchment-scale erosion modelling: a comparison of optimization algorithms. Journal of Hydrology 207, 83–97.

Gan, T.Y., Dlamini, E.M., Biftu, G.F., 1997. Effects of model complexity and structure, data quality, and objective functions on hydrologic modelling. Journal of Hydrology 192, 81–103.

Goldberg, D.E., 1989. Genetic Algorithms in Search, Optimisation, and Machine Learning, Addison-Wesley, Reading, MA, 410p.

Gupta, H.V., Kling, H., Yilmaz, K.K., Martinez, G.F., 2009. Decomposition of the mean squared error and NSE performance criteria: implications for improving hydrological modelling. Journal of Hydrology 377, 80–91.

Gupta, H.V., Sorooshian, S., Yapo, P.O., 1998. Toward improved calibration of hydrologic models: multiple and noncommensurable measures of information. Water Resources Research 34, 751–763.

Gupta, H.V., Wagener, T., Liu, Y., 2008. Reconciling theory with observations: elements of a diagnostic approach to model evaluation. Hydrological Processes 22, 3802–3813.

Hogue, T.S., Sorooshian, S., Gupta, H., Holz, A., Braatz, D., 2000. A multistep automatic calibration scheme for river forecasting models. Journal of Hydrometeorology 1, 524–542.

Hogue, T.S., Gupta, H., Sorooshian, S., 2006. A 'User-Friendly' approach to parameter estimation in hydrologic models. Journal of Hydrology 320, 207–217.
Hreiche, A., Bocquillon, C., Najem, W., Servat, E., Dezetter, A., 2003. Calage d'un modèle conceptuel pluie-débit journalier à partir de bilans annuels. IAHS Publications 278, 87–93.
Kavetski, D., Kuczera, G., Franks, S.W., 2006a. Calibration of conceptual hydrological models revisited: 1. Overcoming numerical artefacts. Journal of Hydrology 320, 173–186.
Kavetski, D., Kuczera, G., Franks, S.W., 2006b. Calibration of conceptual hydrological models revisited: 2. Improving optimization and analysis. Journal of Hydrology 320, 187–201.
Krause, P., Boyle, D.P., Base, F., 2005. Comparison of different efficiency criteria for hydrological model assessment. Advances in Geosciences 5, 89–97.
Kuczera, G., Mroczkowski, M., 1998. Assessment of hydrologic parameter uncertainty and the worth of multiresponse data. Water Resources Research 34, 1481–1489.
Legates, D.R., McCabe, G.J., 1999. Evaluating the use of «goodness of fit» measures in hydrologic and hydroclimatic model validation. Water Resources Research 35, 233–241.
Lin, G.-F., Wang, C.-M., 2007. A nonlinear rainfall–runoff model embedded with an automated calibration method–Part 2: the automated calibration method. Journal of Hydrology 341, 196–206.
Madsen, H., 2000. Automatic calibration of a conceptual rainfall–runoff model using multiple objectives. Journal of Hydrology 235, 276–288.
Madsen, H., Wilson, G., Ammentorp, H.C., 2002. Comparison of different automated strategies for calibration of rainfall–runoff models. Journal of Hydrology 261, 48–59.
Meixner, T., Gupta, H.V., Bastidas, L.A., Bales, R.C., 1999. Sensitivity analysis using mass flux and concentration. Hydrological Processes 13, 2233–2244.
Murphy, A., 1988. Skill scores based on the mean square error and their relationships to the correlation coefficient. Monthly Weather Review 116, 2417–2424.
Nash, J.E., Sutcliffe, J.V., 1970. River flow forecasting through conceptual models. Part 1: A discussion of principles. Journal of Hydrology 10, 2082–2090.
Nelder, J.A., Mead, R., 1965. A simple method for function minimization. Computation Journal 7, 308–313.
New, M.G., Hulme, M., Jones, P.D., 2000. Representing twentieth century space–time climate variability. Part II: Development of 1901–1990 monthly grids of terrestrial surface climate. Journal of Climate 13, 2217–2238.
Perrin, C., Michel, C., Andreassian, V., 2001. Does a large number of parameters enhance model performance? Comparative assessment of common catchment model structures on 429 catchments. Journal of Hydrology 242, 275–301.
Pokhrel, P., Yilmaz, K., Gupta, H.V., 2009. Multiple-criteria calibration of a distributed watershed model using spatial regularization and response signatures. Journal of Hydrology (special issue on DMIP-2).
Romanowicz, R.J., Beven, K.J., 2006. Comments on generalised likelihood uncertainty estimation. Reliability Engineering and System Safety 91, 1315–1321.
Ruelland, D., Ardoin-Bardin, S., Billen, G., Servat, E., 2008. Sensitivity of a lumped and semi-distributed hydrological model to several modes of rainfall interpolation on a large basin in West Africa. Journal of Hydrology 361, 96–117.
Ruelland, D., Guinot, V., Levavasseur, F., Cappelaere, B., 2009. Modelling the long-term impact of climate change on rainfall–runoff processes over a large Sudano–Sahelian catchment. IAHS Publications 333, 59–68.
Ruelland, D., Larrat, V., Guinot, V., 2010. A comparison of two conceptual models for the simulation of hydro-climatic variability over 50 years in a large Sudano–Sahelian catchment. In: Proc. 6th FRIEND International Conference "Global Change: Facing Risks and Threats to Water Resources", Fez, Morocco, 25–29 October 2010, IAHS Publications 340, 668–678.
Schaefli, B., Gupta, H.V., 2007. Do Nash values have value? Hydrological Processes 21, 2075–2080.
Schoups, G., Hopmans, J.W., Young, C.A., Vrugt, J.A., Wallender, W.W., 2005. Multi-criteria optimization of a regional spatially-distributed subsurface water flow model. Journal of Hydrology 311, 20–48.
Schoups, G., Vrugt, J.A., 2010. A formal likelihood function for parameter and predictive inference of hydrologic models with correlated, heteroscedastic, and on-Gaussian errors. Water Resources Research 46, W10531.
Seibert, J., McDonnell, J.J., 2002. On the dialog between experimentalist and modeler in catchment hydrology: use of soft data for multicriterial model calibration. Water Resources Research 38, 1241–1254.
Skahill, B.E., Doherty, J., 2006. Efficient accommodation of local minima in watershed model calibration. Journal of Hydrology 329, 122–139.
Taylor, K.E., 2001. Summarizing multiple aspects of model performance in a single diagram. Journal of Geophysical Research 106, 7182–7183.
Tritz, S., Guinot, V., Jourde, H., 2011. Modelling the behaviour of a karst system catchment using non-linear hysteretic conceptual model. Journal of Hydrology 397, 250–262.
Weglarczyk, S., 1998. The interdependence and applicability of some statistical quality measures for hydrological models. Journal of Hydrology 206, 98–103.
Werth, S., Güntner, A., Petrovic, S., Schmidt, R., 2009. Integration of GRACE mass variations into a global hydrological model. Earth and Planetary Science Letters 277, 166–173.
Winsemius, H.W., Savenije, H.H., Gerrits, A.M.J., Zapreeva, E.A., Klees, R., 2006. Comparison of two model approaches in the Zambezi river basin with regard to model reliability and identifiability. Hydrological Earth Systems Sciences 10, 339–352.
Xiong, L., O'Connor, K.M., 2000. Analysis of the response surface of the objective function by the optimum parameter curve: how good can the optimum parameter values be? Journal of Hydrology 234, 187–207.
Xiong, L., O'Connor, K.M., 2008. An empirical method to improve the prediction limits of the GLUE methodology in rainfall–runoff modelling. Journal of Hydrology 349, 115–124.
Yapo, P.O., Gupta, H.V., Sorooshian, S., 1998. Multi-objective global optimization for hydrologic models. Journal of Hydrology 204, 83–97.